Observation of Young's double-slit interference with the three-photon N00N state

Yong-Su Kim,[1] **Osung Kwon,**[1] **Sang Min Lee,**[2] **Jong-Chan Lee,**[1] **Heonoh Kim,**[2,3] **Sang-Kyung Choi,**[2] **Hee Su Park,**[2,4] **and Yoon-Ho Kim**[1,5]

[1]*Department of Physics, Pohang University of Science and Technology (POSTECH), Pohang, 790-784, South Korea*
[2]*Division of Convergence Technology, Korea Research Institute of Standards and Science, Daejeon, 305-340, South Korea*
[3]*Currently with the Department of Physics, University of Ulsan, Ulsan, 680-749, South Korea*
[4] *hspark@kriss.re.kr*
[5] *yoonho72@gmail.com*

Abstract: Spatial interference of quantum mechanical particles exhibits a fundamental feature of quantum mechanics. A two-mode entangled state of N particles known as N00N state can give rise to non-classical interference. We report the first experimental observation of a three-photon N00N state exhibiting Young's double-slit type spatial quantum interference. Compared to a single-photon state, the three-photon entangled state generates interference fringes that are three times denser. Moreover, its interference visibility of 0.49 ± 0.09 is well above the limit of 0.1 for spatial super-resolution of classical origin.

OCIS codes: (270.0270) Quantum optics; (270.5585) Quantum information and processing; (270.4180) Multiphoton process.

References and links

1. R. P. Feynman, R. B. Leighton, and M. Sands, *The Feynman Lectures on Physics* (Addison Wesley, 1965), Vol. III.
2. Y.-H. Kim, R. Yu, S. P. Kulik, and Y. Shih, "Delayed "choice" quantum eraser," Phys. Rev. Lett. **84**, 1 (2000).
3. U. Sinha, C. Couteau, T. Jennewein, R. Laflamme, and G. Weihs, "Ruling out multi-order interference in quantum mechanics," Science **329**, 418 (2010).
4. J. Jacobson, G. Björk, I. Chuang, and Y. Yamamoto, "Photonic de Broglie wave," Phys. Rev. Lett. **74**, 4835 (1995).
5. A. Ourjoumtsev, H. Jeong, R. Tualle-Brouri, and P. Grangier, "Generation of optical 'Schrödinger cats' from photon number states," Nature **448**, 784 (2007).
6. J. P. Dowling, "Quantum optical metrology—the lowdown of high-N00N states," Contemp. Phys. **49**, 125 (2008).
7. A. N. Boto, P. Kok, D. S. Abrams, S. L. Braunstein, C. P. Williams, and J. P. Dowling, "Quantum interferometric optical lithography: exploiting entanglement to beat the diffraction limit," Phys. Rev. Lett. **85**, 2733 (2000).
8. P. Kok, A. N. Boto, D. S. Abrams, C. P. Williams, S. L. Braunstein, and J. P. Dowling, "Quantum-interferometric optical lithography: Towards arbitrary two-dimensional patterns," Phys. Rev. A **63**, 063407 (2001).
9. V. Giovannetti, S. Lloyd, and L. Maccone, "Quantum-enhanced measurements: Beating the standard quantum limit," Science **306**, 1330 (2004).
10. O. Kwon, Y.-S. Ra, and Y.-H. Kim, "Observing photonic de Broglie waves without the maximally-path-entangled NOON state," Phys. Rev. A **81**, 063801 (2010).
11. J. Fiurášek, "Conditional generation of N-photon entangled states of light," Phys. Rev. A **65**, 053818 (2002).
12. H. Cable and J. P. Dowling, "Efficient generation of large number-path entanglement using only linear optics and feed-forward," Phys. Rev. Lett. **99**, 163604 (2007).
13. K. T. Kapale and J. P. Dowling, "Bootstrapping approach for generating maximally path-entangled photon states," Phys. Rev. Lett. **99**, 053602 (2007).

#154504 - $15.00 USD Received 16 Sep 2011; revised 21 Oct 2011; accepted 14 Nov 2011; published 22 Nov 2011

14. M. D'Angelo, A. Garuccio, and V. Tamma, "Toward real maximally path-entangled N -photon-state sources," Phys. Rev. A **77**, 063826 (2008).
15. K. Edamatsu, R. Shimizu, and T. Itoh, "Measurement of the photonic de Broglie wavelength of entangled photon pairs generated by spontaneous parametric down-conversion," Phys. Rev. Lett. **89**, 213601 (2002).
16. E. J. S. Fonseca, C. H. Monken, and S. Pádua, "Measurement of the de Broglie wavelength of a multi photon wave packet," Phys. Rev. Lett. **82**, 2868 (1999)
17. M. D'Angelo, M. V. Chekhova, and Y. H. Shih, "Two-photon diffraction and quantum lithography," Phys. Rev. Lett. **87**, 013602 (2001).
18. Y. Kawabe, H. Fujiwara, R. Okamoto, K. Sasaki, and S. Takeuchi, "Quantum interference fringes beating the diffraction limit," Opt. Express **15**, 14244 (2007).
19. M. W. Mitchell, J. S. Lundeen, and A. M. Steinberg, "Super-resolving phase measurements with a multiphoton entangled state," Nature **429**, 161 (2004).
20. H. Kim, H.-S. Park, and S.-K. Choi, "Three-photon N00N states generated by photon subtraction from double photon pairs," Opt. Express **17**, 19720 (2009).
21. P. Walther, J.-W. Pan, M. Aspelmeyer, R. Ursin, S. Gasparoni, and A. Zeilinger, "de Broglie wavelength of a non-local four-photon state," Nature **429**, 158 (2004).
22. F. W. Sun, B. H. Liu, Y. F. Huang, Z. Y. Ou, and G. C. Guo, "Observation of the four-photon de Broglie wavelength by state-projection measurement," Phys. Rev. A **74**, 033812 (2006).
23. T. Nagata, R. Okamoto, J. L. O'Brien, K. Sasaki, and S. Takeuchi, "Beating the standard quantum limit with four-entangled photons," Science **316**, 726 (2007).
24. I. Afek, O. Ambar, and Y. Silberberg, "High-N00N states by mixing quantum and classical light," Science **328**, 879 (2010).
25. C. K. Hong, Z. Y. Ou, and L. Mandel, "Measurement of subpicosecond time intervals between two photons by interference," Phys. Rev. Lett. **59**, 2044 (1987).
26. S. J. Bentley and R. W. Boyd, "Nonlinear optical lithography with ultra-high sub-Rayleigh resolution," Opt. Express **12**, 5735 (2004).
27. I. Afek, O. Ambar, and Y. Silberberg, "Classical bound for Mach-Zehnder superresolution," Phys. Rev. Lett. **104**, 123602 (2010).
28. E. Yablonovitch and R. B. Vrijen, "Optical projection lithography at half the Rayleigh resolution limit by two-photon exposure," Opt. Eng. **38**, 334 (1999).
29. A. Yariv and P. Yeh, *Photonics: Optical Electronics in Modern Communications*, 6th ed., (Oxford University Press, 2006).

1. Introduction

Double-slit interference exhibited by single-photons or single-electrons is one of the most fundamental effects in quantum physics and is intimately tied to many foundational concepts in quantum physics such as complementarity, the uncertainty principle, and Born's rule [1–3]. A typical photon number-path entangled state, the N00N state $|\psi\rangle = (|N\rangle_a|0\rangle_b + |0\rangle_a|N\rangle_b)/\sqrt{2}$, where N is the number of quanta and the subscript refers to the spatial mode, naturally arises in generalizing the double-slit experiment to the N-quantum case and was first discussed in the context of photonic de Broglie waves [4]. Such states are of fundamental importance in quantum physics as they represent macroscopic quantum superposition or 'Schrödinger cat' states [5]. Moreover, recent research has shown that the N00N state is at the heart of many quantum-enhanced measurement schemes [6]. For instance, quantum lithography which enables drawing of arbitrary high-contrast patterns with resolution beyond the classical Rayleigh limit requires the N00N state [7,8]. Also, various quantum metrology schemes aimed at achieving the Heisenberg-limited sensitivity are based on the use of the N00N state [9, 10].

Many ideas have been proposed on how to prepare the photonic N00N state [6, 11–14]. Experimental demonstrations of the N00N state, however, have been rather limited. To date, up to five-photon N00N states have been reported in literature [15–24]. However, for four- and five-photon N00N states, experimental demonstrations so far are limited to the measurement-based projection of the N00N state [21–24].

The Young-type double-slit experiment demonstrating spatial quantum interference of the N00N state as originally proposed for quantum lithography, on the other hand, has only been reported for the $N = 2$ N00N state using spontaneous parametric down-conversion (SPDC)

#154504 - $15.00 USD Received 16 Sep 2011; revised 21 Oct 2011; accepted 14 Nov 2011; published 22 Nov 2011

[16–18]. Despite scientific importance, the $N = 2$ case based on SPDC does not offer any resolution breakthrough because it simply retrieves the resolution already obtainable with the pump laser. For truly demonstrating quantum-enhancement of spatial resolution beyond the classical limit, it is essential to show spatial interference fringes for the N00N state with $N \geq 3$. However, all known N00N-related experiments for $N > 2$ reported to date have dealt exclusively with polarization interferometers with a detector fixed in space, thus only exhibiting temporal interference fringes.

In this paper, we report the first experimental demonstration of the Young's double-slit type spatial quantum interference of the three-photon N00N state, exhibiting three times denser spatial interference fringes than that of the single-photon state. This is the first time, to the best of our knowledge, that the spatial quantum interference of the N00N state is observed for more than two photons.

2. Experiment

The schematic of the experimental setup is shown in Fig. 1. First, let us describe the three-photon N00N state generator which is based on Ref. [20]. Pairs of horizontally polarized photons centered at 780 nm are generated at the 2 mm thick type-I BBO crystal via the SPDC process pumped by a femtosecond pump pulse centered at 390 nm, see Fig. 1(a). The pump pulse has a duration of 200 fs and a repetition rate of 76 MHz. The photons of each SPDC pair are then brought back together in a single spatial mode with the help of polarizing beam splitters (PBSs), a quarter-wave plate (QWP1) oriented at 45°, and a movable mirror (M). If the mirror M is set so that the delay time between pairs of SPDC photons is zero, the state becomes

$$|\psi\rangle_{\text{in}} = \left[\gamma a_H^\dagger a_V^\dagger + \frac{\gamma^2}{2} a_H^{\dagger 2} a_V^{\dagger 2} + \frac{\gamma^3}{6} a_H^{\dagger 3} a_V^{\dagger 3} + \cdots\right] |0\rangle\,, \tag{1}$$

where $a_H^\dagger$ ($a_V^\dagger$) denotes the creation operators for a horizontally (vertically) polarized photon. Each term represents single-, double-, and triple-pair emission of SPDC. Our N00N state generation and detection rely on the second term, and the third term contributes to the noise of experimental data, as will be shown later.

The half-wave plate (HWP1) is oriented at 22.5° and the partially-polarizing beam splitter (PPBS) has an amplitude reflection coefficient of $\sqrt{2/3}$ for vertical polarization. The double pairs of $|\psi\rangle_{\text{in}}$ is, then, transformed by passing through the PPBS to become

$$|\psi\rangle = \frac{\sqrt{2}\gamma^2}{6}\left[a_{V1}^\dagger \otimes \left(\frac{1}{3} a_{V2}^{\dagger 3} - a_{H2}^{\dagger 2} a_{V2}^\dagger\right)\right]|0\rangle + \left[\frac{1}{8} a_{H2}^{\dagger 4} - \frac{1}{12} a_{H2}^{\dagger 2} a_{V2}^{\dagger 2} + \frac{1}{72} a_{V2}^{\dagger 4}\right]|0\rangle + |\text{etc}\rangle, \tag{2}$$

the subscripts 1 (2) refers to the reflected (transmitted) mode of the PPBS [20]. Note that, in Eq. (2), the four-photon amplitudes that do not result in at least three photons in mode 2 are expressed as $|\text{etc}\rangle$ and they do not contribute to the $N = 3$ N00N state interference as they cannot be registered at the three-photon detector.

The first term in Eq. (2) is now relevant to our purpose: if a single-photon detection occurs at the single-photon counter SPC1, the three-photon state in mode 2 after QWP2 oriented at 45° is given as

$$|\psi\rangle_p = (|3\rangle_H|0\rangle_V + i|0\rangle_H|3\rangle_V)/\sqrt{2}. \tag{3}$$

In other words, the three-photon polarization N00N state $|\psi\rangle_p$ is heralded in mode 2 (at the entrance of the single mode fiber SMF) whenever there is a single-photon detection at SPC1 [20]. A three-photon absorber located at mode 2, if followed by a shutter triggered by SPC1, would be able to record genuine three-photon quantum interference fringes due to the N00N state.

#154504 - $15.00 USD Received 16 Sep 2011; revised 21 Oct 2011; accepted 14 Nov 2011; published 22 Nov 2011

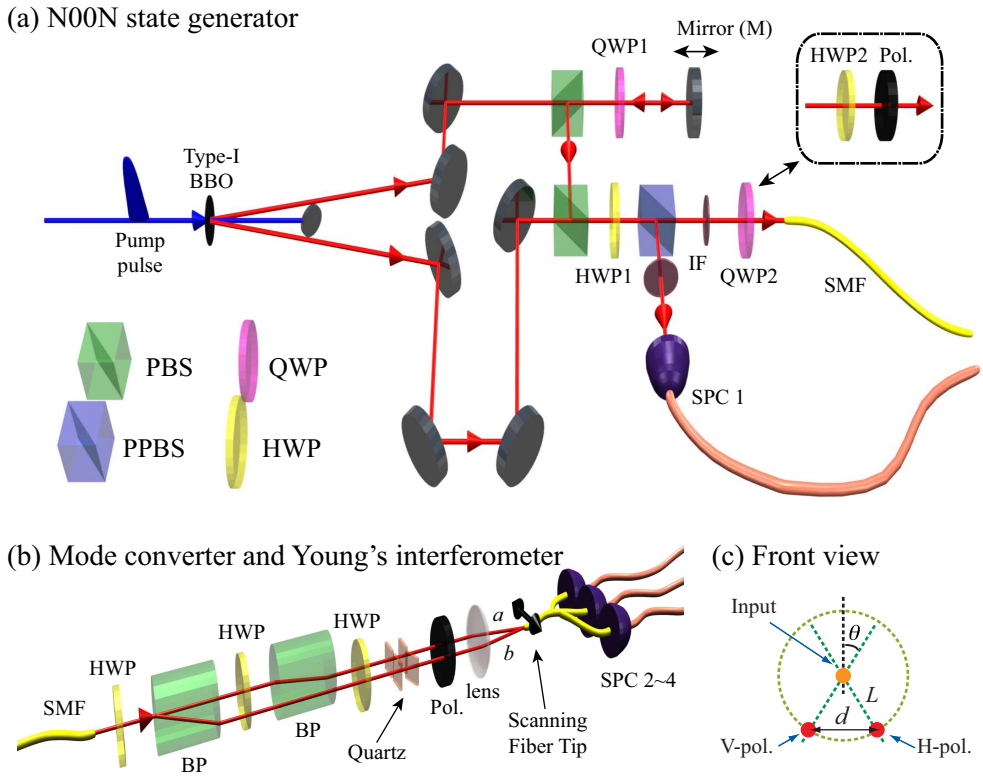

Fig. 1. Schematic of the experimental setup. (a) The polarization N00N state $|\psi\rangle_p$ is prepared in a single spatial mode. IF is an interference filter with full-width at half-maximum bandwidth of 5 nm at SPC1 (10 nm at SMF) centered at 780 nm. (b) Mode converter which losslessly transforms $|\psi\rangle_p$ to $|\psi\rangle_s$ and Young-type double-slit interferometer. (c) Front view of the mode converter.

Finally, the polarization N00N state $|\psi\rangle_p$ is transformed to the spatial two-mode three-photon N00N state $|\psi\rangle_s$,

$$|\psi\rangle_s = (|3\rangle_a|0\rangle_b + |0\rangle_a|3\rangle_b)/\sqrt{2}, \tag{4}$$

by using the mode converter shown in Fig. 1(b) and 1(c). The mode converter, which consists of half-wave plates (HWP), birefringent prisms (BP), quartz plates, and a polarizer (Pol), is based on the following operation principle. The first and second BPs are aligned so that their optic axes are oriented respectively at $+\theta$ and $-\theta$ with respect to the vertical polarization. The first two HWPs are used for rotating the horizontal-vertical polarization basis of the photons so that they overlap with the rotated optic axes of BPs. The third HWP and the quartz plates are used to match the polarization states of photons in spatial modes a and b. An additional horizontal polarizer (Pol) is used to clean up the polarization state so that all three photons in Eq. (4) are guaranteed to have the same polarization.

The spacing $d = 2L\sin\theta$ between the modes a and b is determined by the angle θ and the beam walk-off (i.e., e- and o-ray separation) L of a single BP (see Fig. 1(c)). In the experiment, considering the numerical aperture (0.12) and mode field diameter (5.6 μm) of SMF, the $1/e^2$ beam diameter of each spatial mode is estimated to be 1.4 mm. The beam spacing d was chosen

#154504 - $15.00 USD Received 16 Sep 2011; revised 21 Oct 2011; accepted 14 Nov 2011; published 22 Nov 2011

as $d = 2.2$ mm, which leads to a mode overlap of 0.8 %. Our mode converter design provides excellent interferometric phase stability between the spatial modes *a* and *b*.

To observe the double-slit interference fringes of the three-photon N00N state $|\psi\rangle_s$, a single-mode fiber (identical to SMF) tip was scanned at the focus of a lens (15 mm focal length) by using a piezo-controlled translation stage, see Fig. 1(b). The group delay between the spatial modes *a* and *b* was compensated by a set of mirrors (not shown in the figure) in front of the focusing lens. The other end of the fiber tip was connected to three single-photon detectors (SPC2∼4) via a set of 3 dB fiber beamsplitters. The three-fold coincidence SPC2–SPC3–SPC4 triggered by SPC1 constitutes the proper measurement for the heralded three-photon N00N states, $|\psi\rangle_p$ and $|\psi\rangle_s$.

3. Temporal interference of three-photon N00N state

The quality of the polarization N00N state $|\psi\rangle_p$ is directly responsible for the quality of the spatial N00N state $|\psi\rangle_s$, which in turn affects the double-slit interference visibility with $|\psi\rangle_s$. Hence, it is of utmost importance to ensure that the three-photon polarization N00N state is prepared with high purity. Thus, we have first measured the temporal interference fringes due to $|\psi\rangle_p$ as in other N00N state experiments [10, 15, 19–24].

The first step in preparing the three-photon N00N state is to ensure that photons arrive at the second PBS simultaneously. This can be done by observing the Hong-Ou-Mandel (HOM) interference between detectors SPC1 and SPC2 while scanning the mirror M [20, 25]. In the experiment, we observed the HOM dip with 95.4% visibility at 70 mW pump power.

The heralded three-photon state just before QWP2 is the N00N state composed of the left- and right-circularly polarized three-photon states. Thus, to observe temporal quantum interference due to $|\psi\rangle_p$, we replace QWP2 with a HWP2 and a horizontal polarizer (Pol.) as shown inset of Fig. 1(a) and connect the output end of SMF to the fiber-coupled three-photon detector (SPC2–SPC3–SPC4) depicted in Fig. 1(b). It is then possible to introduce a phase difference χ between the left-circular and right-circular polarization modes of $|\psi\rangle_p$ by rotating HWP2 by $\chi/4$ and the temporal N00N state interference can be observed in four-fold coincidences between the trigger detector and the three-photon detector. The experimental data for the temporal interference measurements are shown in Fig. 2. The error bars denote statistical uncertainty calculated as square root of the measured counts. We first measured, as a reference, the heralded single-photon interference shown in Fig. 2(a). In Fig. 2(b), the response of the three-photon detector, three-fold coincidences among SPC2–SPC3–SPC4, is shown. In this case, the first two terms of Eq. (2) affect the outcome and the three-fold coincidence probability *P* is calculated to be

$$P \propto \eta^3\gamma^4\,[4\sin^2(3\chi/2) + 8(\sin(\chi)+\sin(2\chi))^2 + (2-\eta)(1+2\cos(\chi))^4], \tag{5}$$

where it is assumed that the three-photon detector consists of three single-photon detectors connected with 3 dB fiber beamsplitters as shown in Fig. 1(b) and η is the detection efficiency at each detector. The first term is due to the heralded three-photon N00N state term, i.e., the first term in Eq. (2), and the second/third terms are from the second term in Eq. (2). The amplitudes expressed as $|\text{etc}\rangle$ in Eq. (2) do not contribute to the outcome of the three-photon detector. The experimental data in Fig. 2(b) is in good agreement with the above theoretical calculation.

In Fig. 2(c), we show the heralded three-photon N00N state interference observed in four-fold coincidences. The data, however, is affected by the coincidences due to non-N00N state terms, i.e., 2nd and 3rd terms in Eq. (5) when higher order emission of SPDC shown in Eq. (1) is present. The major noise appears at the phase difference of multiples of 360 degree as shown in Fig. 2(c). At these points, double-pair emission cannot result in the four-fold coincidence, and the four-fold coincidence probability due to triple-pair generation of SPDC equals the single

#154504 - $15.00 USD Received 16 Sep 2011; revised 21 Oct 2011; accepted 14 Nov 2011; published 22 Nov 2011

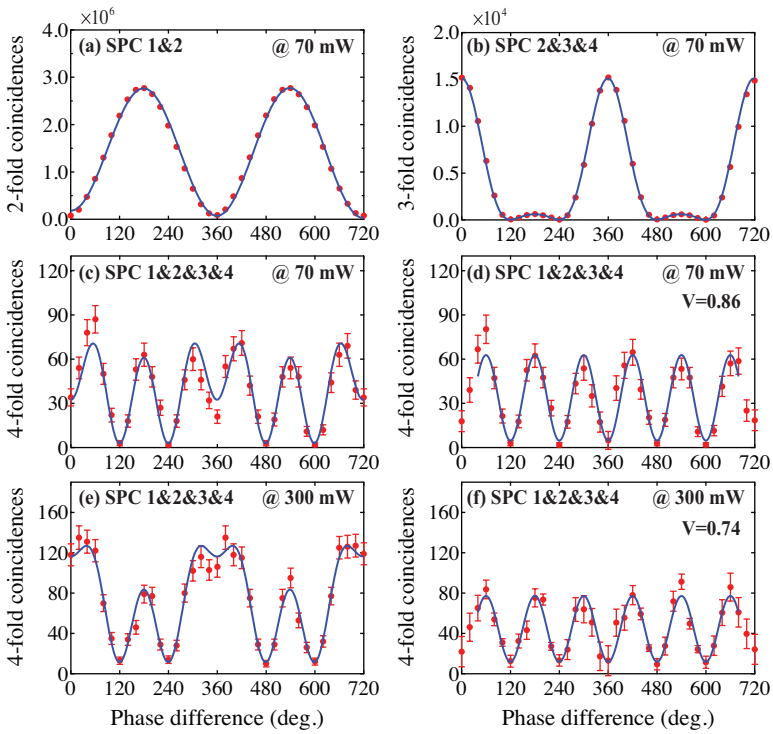

Fig. 2. Temporal fringes observed in (a) 2-fold coincidences between SPC1–SPC2, (b) 3-fold coincidences among SPC2–SPC3–SPC4, and (c) $\sim$ (f) 4-fold coincidences. The heralded single-photon state interference is shown in (a). The heralded three-photon N00N state interference shown in (c) and (e) are degraded by noise counts due to the triple-pairs from SPDC. The noise-subtracted three-photon N00N state interference, (d) and (f), show the three-times faster modulation frequency compared to the single-photon interference shown in (a). The data acquisition times (for each data point) are 1200 s for (a) $\sim$ (d) and 100 s for (e) and (f). Solid lines are fitting curves based on Eq. (5).

photon detection probability at SPC1 multiplied by the unheralded three-photon coincidence probability. We calculate this product of the two probabilities over all the data and subtract from the raw data in Fig. 2(c). When this approximate contribution of the triple-pair emission is subtracted, the four-fold coincidence shown in Fig. 2(d) exhibits high-visibility ($V = 0.86 \pm 0.08$) heralded three-photon N00N state interference with three-times greater phase resolution than the single-photon case shown in Fig. 2(a). Even at a much higher pump power of 300 mW, similar results are observed, see Fig. 2(e) and Fig. 2(f), albeit with somewhat reduced visibility ($V = 0.74 \pm 0.07$). Note that the background noise by triple-pairs at 300 mW pump power is much larger than it of at 70 mW pump power since as we increase the pump power, the SPDC efficiency amplitude γ also increases. The observed three-photon N00N state visibilities after the background noise subtracted, however, are well above the classical limit of 0.1 either in 70 mW or 300 mW of pump power [26, 27].

Note that we can minimize these unwanted noise effects by lowering the pump power. In our experiment, however, we conduct the experiment at high pump power to get higher count rate. Under our purpose of the experiment, a proof of principle experiment, it is okay since even with a high pump power, we can get sufficient visibility which is well above the classical limit after the noise subtraction.

#154504 - $15.00 USD Received 16 Sep 2011; revised 21 Oct 2011; accepted 14 Nov 2011; published 22 Nov 2011

4. Spatial interference of three-photon N00N state

Having confirmed that the three-photon polarization N00N state, $|\psi\rangle_p$, is prepared with sufficiently high purity, we now proceed to demonstrate the Young's double-slit interference with the N00N state $|\psi\rangle_s$. For this measurement, QWP2 is now restored at its original location and the $|\psi\rangle_p$ is transformed to the $|\psi\rangle_s$ state with the mode converter shown in Fig. 1(b). Spatial interference fringes are measured with the detection scheme also shown in Fig. 1(b) and the pump power is increased to 400 mW.

The experimental data for the double-slit interference of the three-photon N00N state $|\psi\rangle_s$ are shown in Fig. 3. As was in the temporal interference data, the error bars are the standard deviations which correspond to the square roots of the measured counts. We first measured the spatial profile of the beam at the focus of the lens by blocking mode *b*. The single-photon and the three-photon spatial profiles are shown in Fig. 3(a) and Fig. 3(b), respectively. Note that both the single-photon and the three-photon states are heralded by single-photon detection at SPC1. Fitting the data with a Gaussian function $\exp[-(x/w_0)^2]$, we find that the $2w_0$ widths are 10.8 ± 0.4 μm for the single-photon case and 6.2 ± 0.6 μm for the three-photon case. This is in good agreement with the theoretical estimation that the three-photon probability distribution is

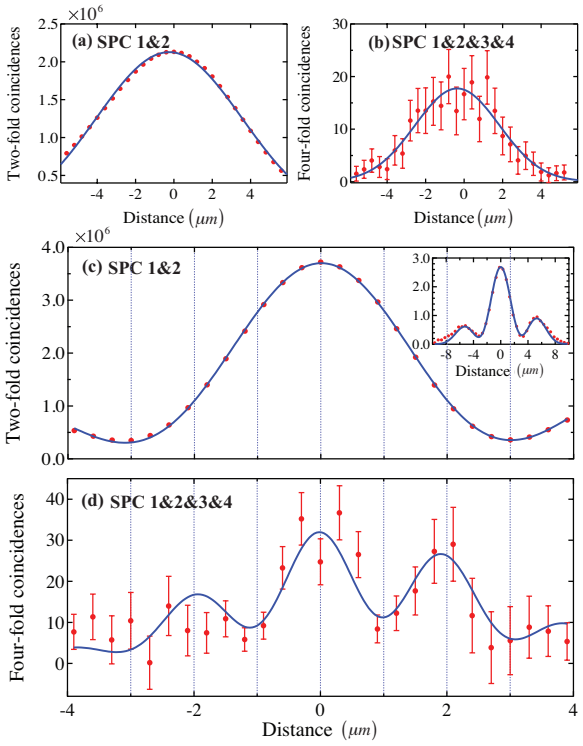

Fig. 3. Spatial profile of the heralded (a) single-photon state and (b) three-photon state for a single beam (no interference). The data accumulation time is 3400 s for each point and solid lines are Gaussian fits to the data. Interference of the heralded single-photon state and the heralded three-photon N00N state are shown in (c) and in (d), respectively. The data were accumulated for 1700 s each point. Solid lines are fitting curves based on theoretical calculation. The noise contributions have been subtracted. The $|\psi\rangle_s$ state exhibits three times faster spatial interference fringes (2.0 μm) than that of the single-photon state (6.0 μm).

#154504 - $15.00 USD Received 16 Sep 2011; revised 21 Oct 2011; accepted 14 Nov 2011; published 22 Nov 2011

proportional to the cube of the single-photon one.

For the Young-type double-slit interference measurement, both modes *a* and *b* are now open and interference fringes are measured in two-fold and four-fold coincidences at the focus of the lens as a function of the scanning fiber tip position, see Fig. 3(c) and Fig. 3(d). The fitting curves are Gaussian envelops multiplied by a raised sine curve. The size of Gaussian envelop is obtained from the spatial profile without interference shown in Fig. 3(a) and Fig. 3(b). Here the visibility is calculated from the offset and amplitude of the sinusoidal modulation. In theory, the fringe patterns are expected to show sinusoidal modulations within the respective spatial profiles of the single- and three-photon states and the modulation frequency for the three-photon N00N state should be three times more than that of the single-photon state. The experimental data, which show fringe spacing of 6.0 μm for the single-photon state and 2.0 μm for the three-photon N00N state, are thus in good agreement with the theory. We point out that, although the mode field diameter of the scanning fiber tip is larger than the fringe spacing due to the three-photon N00N state, the fact that the fiber is single-mode at 780 nm allows us to measure a spatial fringe spacing smaller than the mode field diameter without sacrificing the visibility. See the Appendix for details.

The asymmetry in both the single- and three-photon interference is due to a non-zero phase difference of the interfering two beams at the beam center. This phase difference can also be measured by comparing the magnitude of two sidebands. From the single-photon interference measurement before and after the three-photon measurement for 13 hours shown in Fig. 3(d), the phase drift estimated to be 0.01 rad, which confirms the stability of our spatial interferometer.

In general, spatial super-resolution itself may not necessarily be of quantum origin [28]. However, the fringe visibility V is an important feature that distinguishes between quantum and classical cases. For three-photon Young's double-slit interference, the classical limit of the fringe visibility can be calculated by considering detection of the intensity cubed (i.e., three-photon detection) rather than detection linear in intensity (i.e., single-photon detection) and has been shown to be 0.1 [26, 27]. In this work, the double-slit interference with the three-photon N00N state exhibits $V = 0.49 \pm 0.09$ which is well above the classical limit of 0.1.

5. Conclusion

These experimental results are the first demonstration of the Young-type double-slit interference of the three-photon N00N state. Our work demonstrates clearly both spatial super-resolution and fringe visibility surpassing the classical limit. This is the first time that the spatial quantum interference of the N00N state is observed for more than two photons, thus paving the way towards new applications in quantum metrology, quantum imaging, and quantum interferometric lithography.

Appendix : Spatial interference measurement with a single mode fiber

Consider the experimental setup shown in Fig. 4(a) where two beams of light are brought together by a lens. At the focus of the lens, the two beams overlap and interference takes place. The spatial interference fringe pattern (intensity profile) has the fringe spacing of l and the envelope profile of $2\sigma_x$, see the inset in Fig. 4(a).

Suppose that interference fringe is measured with a detector connected to a single-mode fiber (SMF) scanned in the transverse plane. The coupling efficiency η_k of an incident beam to a resonator or an optical fiber is

$$\eta_k \sim \sum_k \left| \int E_{\rm in}(x,y) E_k^*(x,y) dx dy \right|^2 , \tag{6}$$

#154504 - $15.00 USD Received 16 Sep 2011; revised 21 Oct 2011; accepted 14 Nov 2011; published 22 Nov 2011

where $E_{\text{in}}(x,y)$ and $E_k(x,y)$ refer to the electric field of the incident beam at the input plane and the wave function of the resonator (or fiber) mode, respectively [29]. The electric field $E_{\text{in}}(x,y)$ at the location of the SMF tip shows interference and it can be written as

$$E_{\text{in}}(x,y) \sim \sin(fx+\phi)\ \exp\left[-\left(\frac{x}{\sigma_x}\right)^2\right] \exp\left[-\left(\frac{y}{\sigma_y}\right)^2\right], \tag{7}$$

where $2\sigma_x$ ($2\sigma_y$) denotes the horizontal (vertical) envelope. Furthermore, it is well known that SMF guides only one spatial mode that can be approximately described as a Gaussian (known as LP01 or HE11 mode),

$$E_0(x,y) \sim \exp\left[-\left(\frac{x-\Delta}{\sigma}\right)^2\right] \exp\left[-\left(\frac{y}{\sigma}\right)^2\right], \tag{8}$$

where 2σ is the mode field diameter of the SMF and Δ is a position of the scanning SMF.

Inserting Eq. (8) and (7) to (6) yields the spatial interference pattern measured by the SMF. An notable result is that the spatial interference is measurable even when the spatial fringe spacing l is smaller than the mode field diameter 2σ. To demonstrate that such a measurement is indeed possible, we set up the Young's interferometer with a He-Ne laser as shown in Fig. 4(a). By varying the beam size d and the beam spacing L, we are able to change the interference envelope $2\sigma_x$ as well as the fringe spacing l. The mode field diameter of SMF used in our experiment is $2\sigma = 5.4\,\mu m$.

We first test the measurement setup with $l = 39.8\,\mu m > 2\sigma = 5.4\,\mu m$ and the result is shown in Fig. 4(b). The fringe is clearly resolved with the visibility of 0.82. We now vary L such that the expected fringe spacing $l = 1.9\,\mu m$, smaller than the mode field diameter of SMF. The

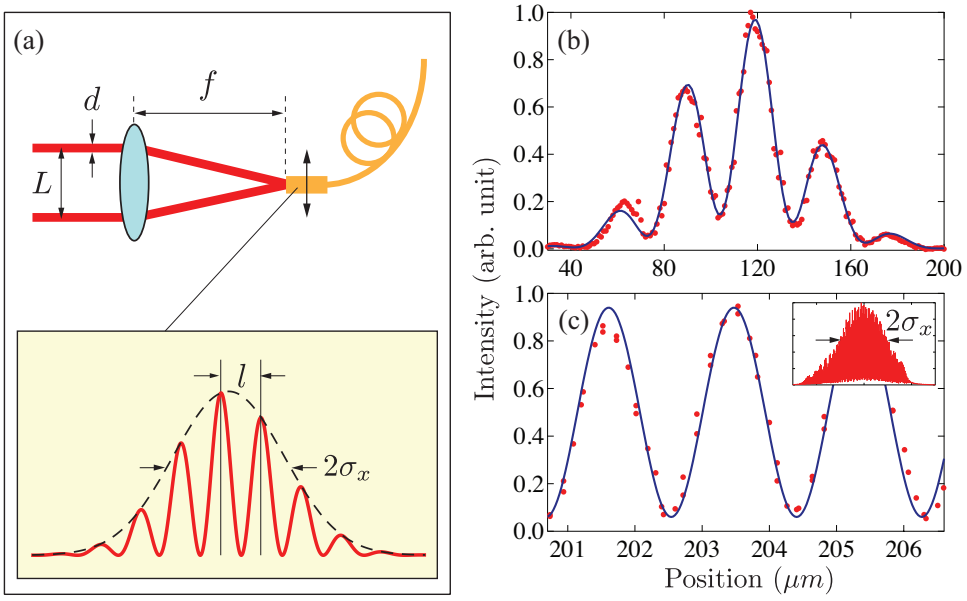

Fig. 4. (a) Setup for measuring fringes of a Young's interferometer. (b) The fringe spacing l is larger than the mode field diameter of SMF 2σ; $l > 2\sigma$. (c) The fringe spacing l is smaller than the mode field diameter of SMF 2σ; $l < 2\sigma$. The inset shows an overall interference envelope.

#154504 - $15.00 USD Received 16 Sep 2011; revised 21 Oct 2011; accepted 14 Nov 2011; published 22 Nov 2011

experimental data are shown in Fig. 4(c) and the visibility is better than 0.89. It is clear that, due to the overlap integral of Eq. (6), we are able to measure fringe spacing smaller than the mode field diameter of SMF.

For the three-photon detection setup shown in Fig. 1(b), the coupling efficiency is given as

$$\eta_k \sim \left| \int \Psi_{\text{in}} E_k^*(x_1,y_1) E_k^*(x_2,y_2) E_k^*(x_3,y_3) dx_1 dy_1 dx_2 dy_2 dx_3 dy_3 \right|^2, \tag{9}$$

where Ψ_{in} denotes the incident field. Thus, the three-photon envelope will be reduced by the factor of $\sqrt{3}$ compared to the single-photon envelope. However, the main result of the previous analysis still holds and spatial interference is measurable even when the fringe spacings are smaller than the envelope.

Acknowledgments

This work was supported by the National Research Foundation of Korea (2009-0070668 and 2009-0084473) and the KRISS Single-Quantum-Based Metrology in Nanoscale Project. YSK acknowledges the support of the Korea Research Foundation (KRF-2007-511-C00004).

#154504 - $15.00 USD Received 16 Sep 2011; revised 21 Oct 2011; accepted 14 Nov 2011; published 22 Nov 2011